

Accelerated Aging of SiC Coating: Numerical and Experimental Study



Presented by :

Thiane NDIAYE 2nd year PhD student at PROMES, France

Supervisors:

Ludovic CHARPENTIER researcher, PROMES-CNRS

Reine REOYO-PRATS lecturer UPVD, PROMES-CNRS

Collaboration:

Frédéric MERCIER researcher, SIMaP (CNRS/UGA/Grenoble INP)

Plan

Introduction

Materials

Methods

Results and Discussion

Conclusion and Perspectives

Context: Concentrated Solar Technologies (CST)

- Conversion of solar energy → thermal energy → electricity or heat
- Low Efficiency (~16%) due to moderate operating temperature (~600 °C)
- Bottleneck: mechanical and oxidation limits of the receiver

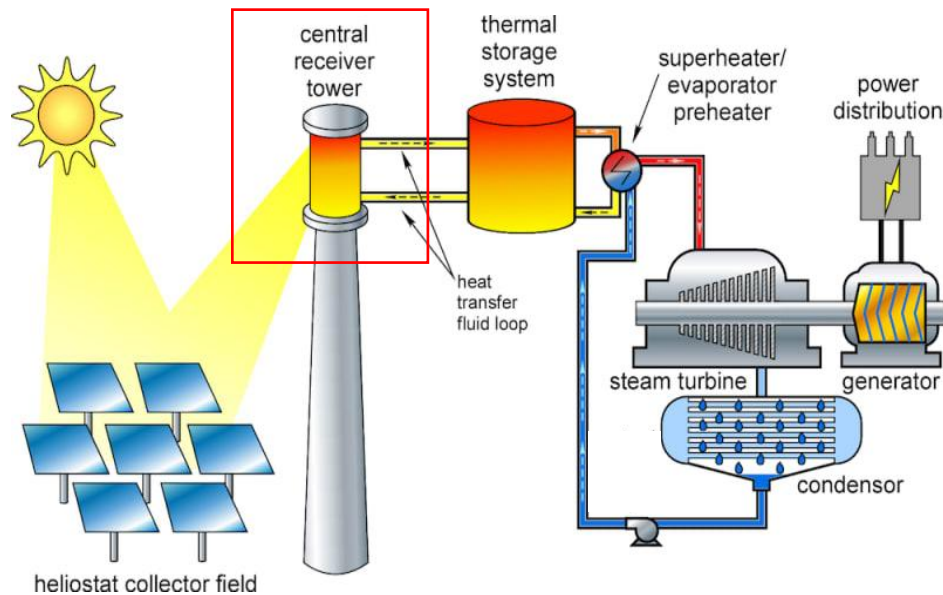
Objectives:

- **Operating at higher temperatures > 1000 °C**

- ✓ Front side → exposed to concentrated solar flux (1000 kW/m²)
- ✓ Rear side → thermal exchange with heat transfer fluid

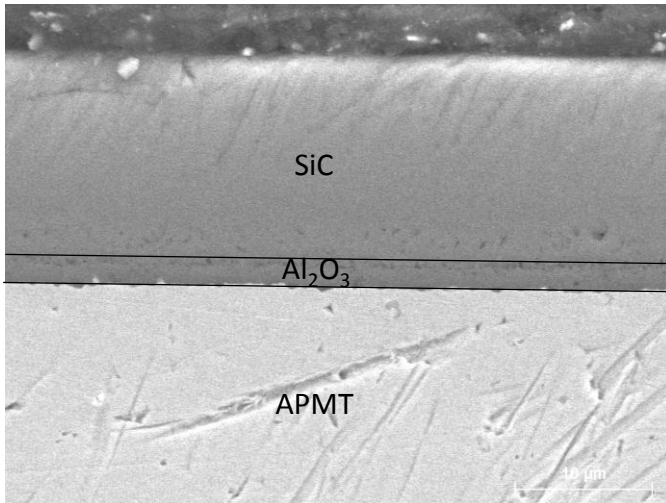
- **Design of a high-performance receiver:**

- ✓ Oxidation resistant
- ✓ Good creep resistance and thermal cycling durability
- ✓ Retention of optical properties



□ Proposed Approach:

- Receiver made of a metal alloy coated with ceramic layers:
 - ✓ Alloy provides mechanical strength
 - ✓ Ceramic enhances solar-to-thermal conversion efficiency



□ Methodology:

- **Numerical simulation:** estimation of stresses
 - ✓ APMT oxidation
 - ✓ SiC deposition
 - ✓ Thermal cycling
- **Experimental test under solar flux:**
 - ✓ Cycling under solar flux
 - ✓ Temperature evaluation
- **Comparison of numerical and experimental approaches:**
 - ✓ Improvement of the numerical model
 - ✓ Optimization of the multilayer structure

□ Substrate layer: Kanthal APMT (Fe-bal-Cr₂₁₋₂₂-Al₅-Mo₃)

- Creep-resistant up to **1250 °C**
- Oxidation-resistant (FeCrAl alloy)

□ Intermediate Layer: Alumina (Al₂O₃)

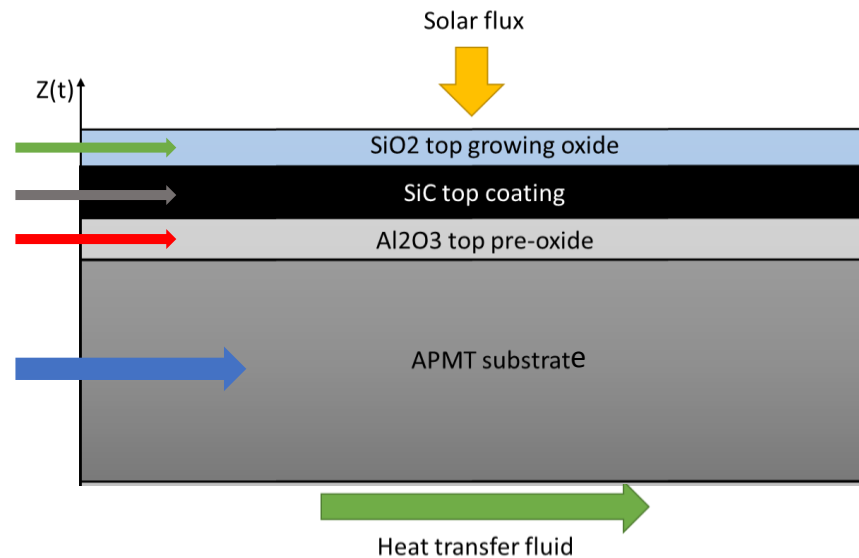
- Substrate oxidation prior to deposition
- Facilitates accommodation of SiC
- High Thermal stability up to **1700 °C**

□ Coating layer: Cubic Silicon carbide (SiC)

- **HT-CVD** (High-Temperature Chemical Vapor Deposition)
- at **1200 °C** : SiH₄ and C₃H₈
- Oxidation resistance
- High Solar absorptivity ~80%

□ Oxidation of SiC into SiO₂ during thermal cycling

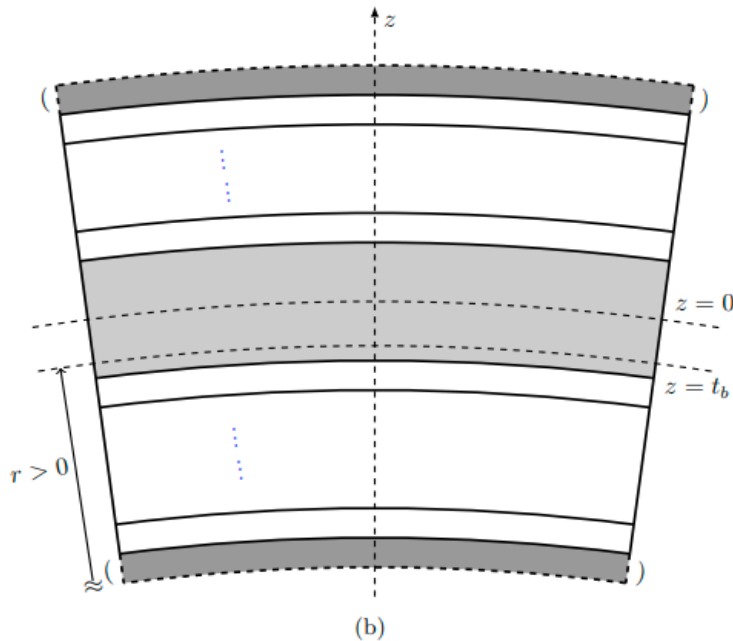
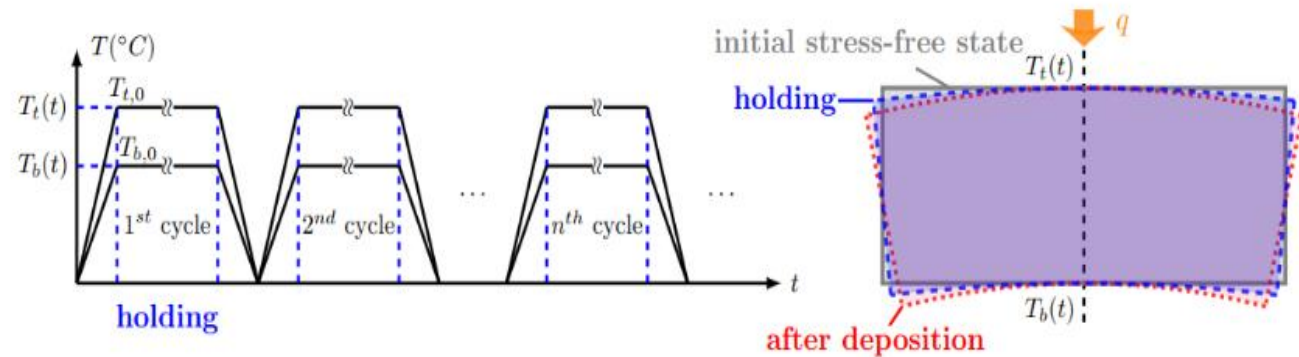
- Growing protective oxide layer



Properties	Fe-Cr-Al-Mo	Al ₂ O ₃	3C-SiC	SiO ₂
Young Modulus E (GPa)	220	379	430	50-60
Poisson ratio ν	0.3	0.25	0.16	0.17
Density (g.cm ⁻³)	7.25	3.87	3.21	2.65
Thermal conductivity (W m ⁻¹ K ⁻¹) à 1000 °C	27	10	21	1.6-1.2
Thermal expansion (10 ⁻⁶ K ⁻¹)	15.5	8	5	0.55-0.6

□ 1D Model in MATLAB

- Simulates thermal aging through cycling (room temperature ↔ 1000 °C)
- Calculates:
 - ✓ Temperature through layers
 - ✓ Different strains
 - ✓ Stresses in different layers



□ Base on Hsueh Model: calculates the strain $\epsilon(z) = c + \frac{z-t_b}{r}$

- c : uniform strain component
- $\frac{z-t_b}{r}$: bending strain component where t_b is the bending axis position,
- $\frac{1}{r}$: the curvature and z is the position in layers

□ Stress in layers

- Stress in substrate: $\sigma_s(z) = \frac{E_s}{1-\nu_s} \left(c + \frac{z-t_b}{r} - \varepsilon_{s,thermal} - \varepsilon_{s,coating} - \varepsilon_{s,thermal} - \varepsilon_{s,creep} \right)$
- Stress in other layers: $\sigma_{layer}(z) = \frac{E_{layer}}{1-\nu_{layer}} \left(c + \frac{z-t_b}{r} - \varepsilon_{layer,coating} - \varepsilon_{layer,thermal} - \varepsilon_{layer,creep} \right)$
 - ✓ Coating : due to deposition
 - ✓ Thermal: due to thermal expansion
 - ✓ Creep: due to temperature holding
- In order to obtain **the stresses**, one must solve a system of equations involving three unknowns (**c, t_b, and r**):
 - ✓ The sum of the forces due to the uniform deformation **equal to zero**
 - ✓ The sum of the forces due to the bending experienced by the sample **equal to zero**
 - ✓ The resultant moment with respect to the axis of curvature **equal to zero**

□ Experimental Setup: SAAF (Solar Accelerated Aging Facility)

➤ Main Components

- **Solar concentration system:**

- ✓ Mobile heliostat (6 m × 4.5 m) → tracks the sun
- ✓ Fixed parabolic mirror (Ø 1.5 m, 900 W power, concentrates 15,000 times)
- ✓ Focal point: Ø ~20 mm at 635 mm from center

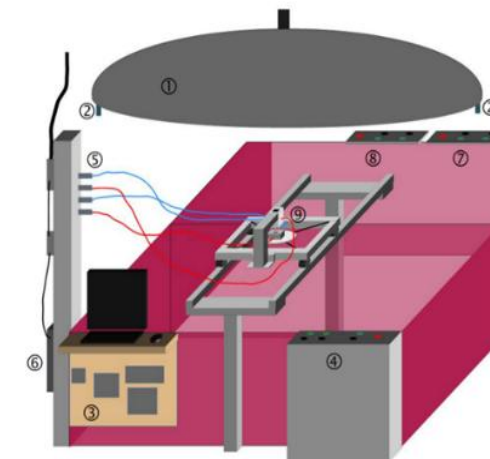
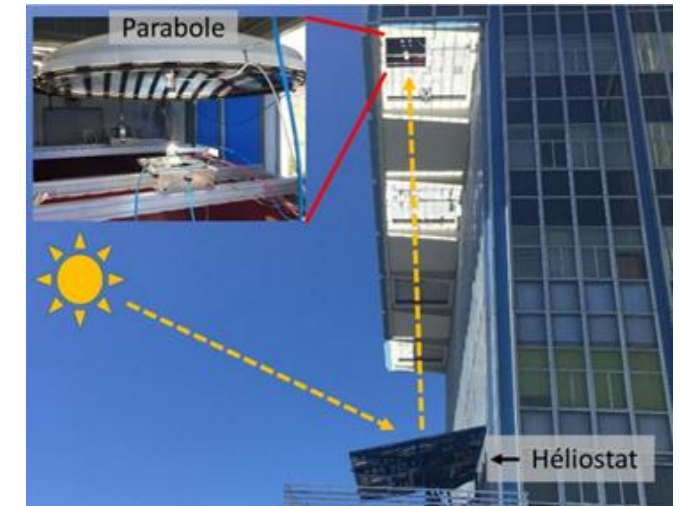
- **Kaleidoscope:** homogenizes the flux on the sample

- **Movable shutters (blades):** control the solar flux

- **Cooling:** water (kaleidoscope) and compressed air (sample holder)

- **Control system and data acquisition**

➤ Usage: Simulate multilayer aging through controlled thermal cycling



1. Parabolic dish reflector
2. Laser
3. Control panel
4. Control console (S/E trapdoor)
5. Cooling ball valves
6. Air flowmeter
7. Control console (tracking)
8. Control console (S/W trapdoor)
9. Experimental cart

Residual Stress Measurement by X-ray Diffraction (XRD)

XRD $\sin^2\psi$ Method:

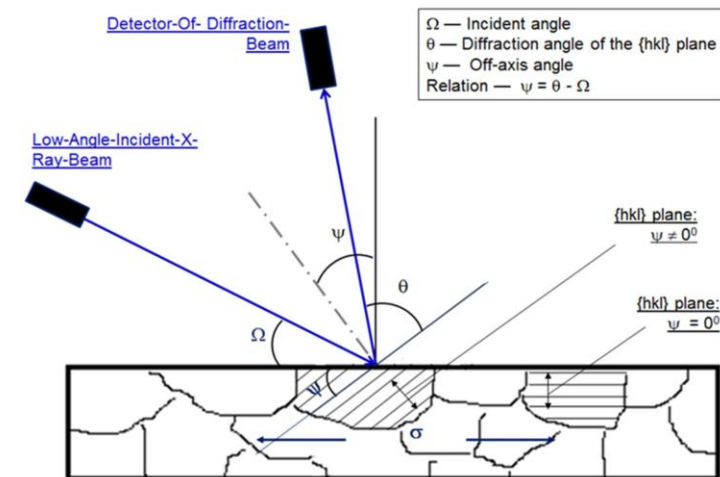
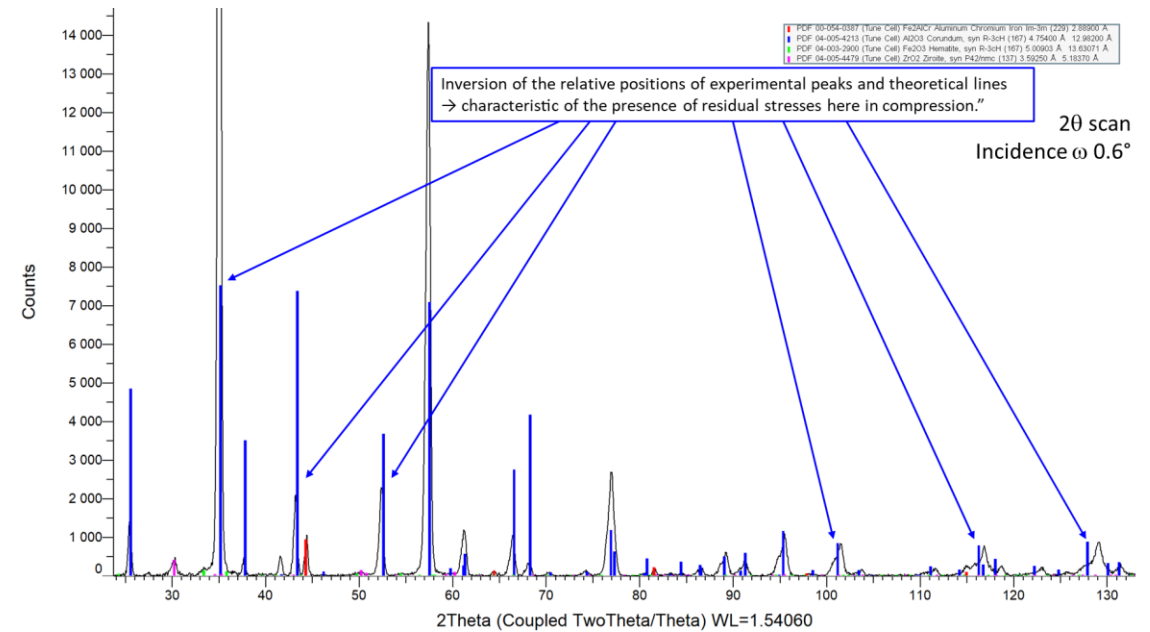
- Uses crystalline planes as strain gauges
- **Measures d-spacing at different ψ angles**
- Linear plot (ε vs $\sin^2\psi$) \rightarrow slope gives residual stress

Limitations of Conventional Method:

- High diffraction angles ($2\theta > 125^\circ$) usually required
- Problematic for thin films: weak and broadened peaks

Alternative: GIXRD (Glancing Incident XRD):

- Employs a constant, low incident angle Ω
- Different ψ angles obtained via $\psi = \theta - \Omega$
- Especially suited for thin films and surface layers
- Effective for cubic crystalline materials

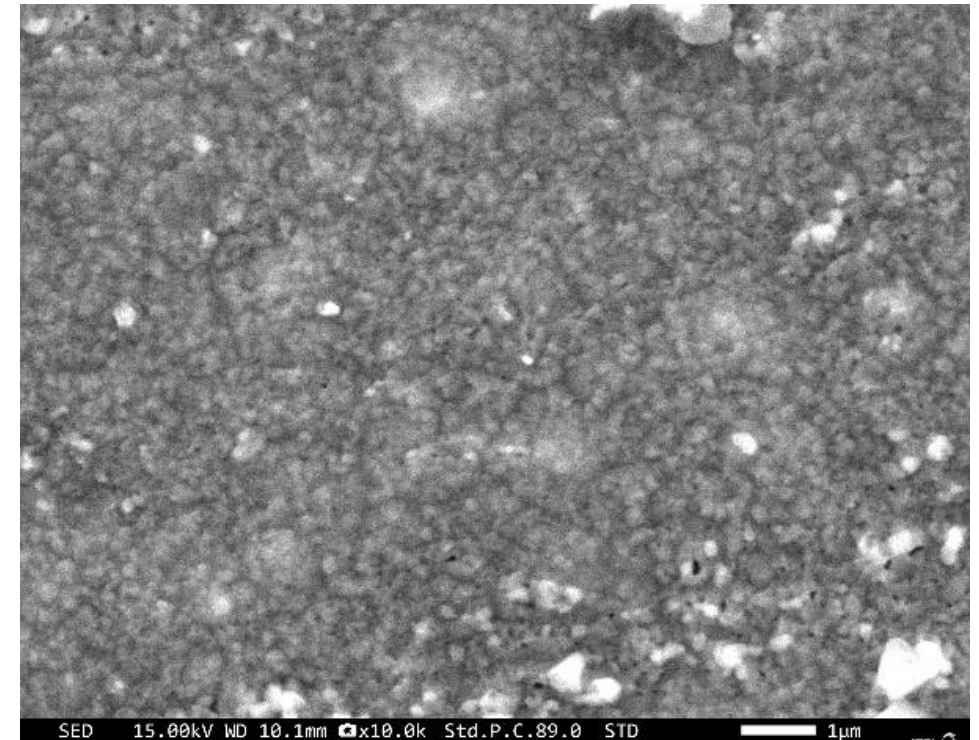


□ After oxidation : stresses in Al_2O_3 /APMT sample

- Treatment: **50 hours at 1100 °C in air**
- Aluminum oxide formed : **$\alpha\text{-Al}_2\text{O}_3$**
- Homogeneous surface
- No cracking observed

Layer	Numerical (MPa)	Experimental (MPa)	Limit compressive strength (MPa)
Al_2O_3	-2489.7	-2760	-2000 to -4000

- Compressive in both methods
- Values very close (<10%)
- The model accurately represents the oxidation process

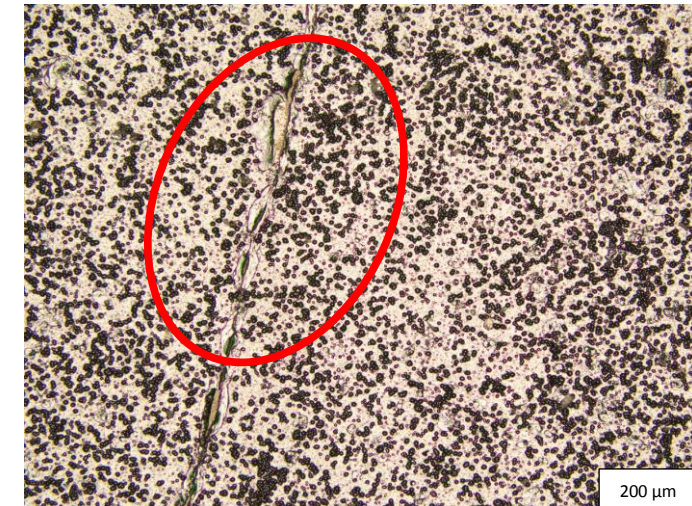
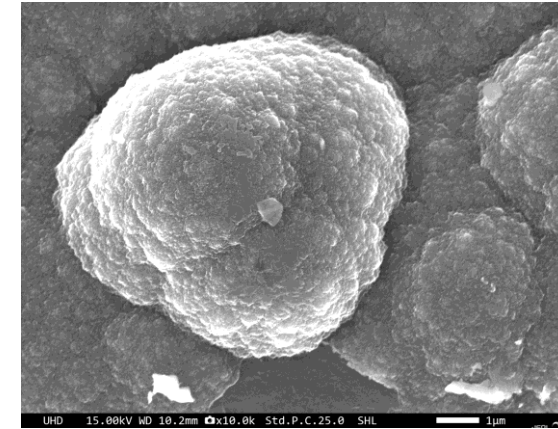
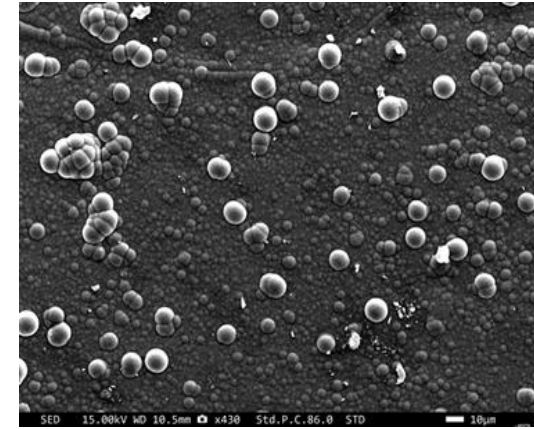


□ After SiC deposition : stresses in SiC/Al₂O₃/APMT simple

- **SEM image:** “Cauliflower” morphology, typical of HTCVD 3-SiC
- Some coating delamination observed along the existing scratches in the substrate.

Layer	Numerical (MPa)	Experimental (MPa)	Limit compressive strength (MPa)
SiC	-1845	-2393	2500-3500
Al ₂ O ₃	-2967	-3120	2000-4000

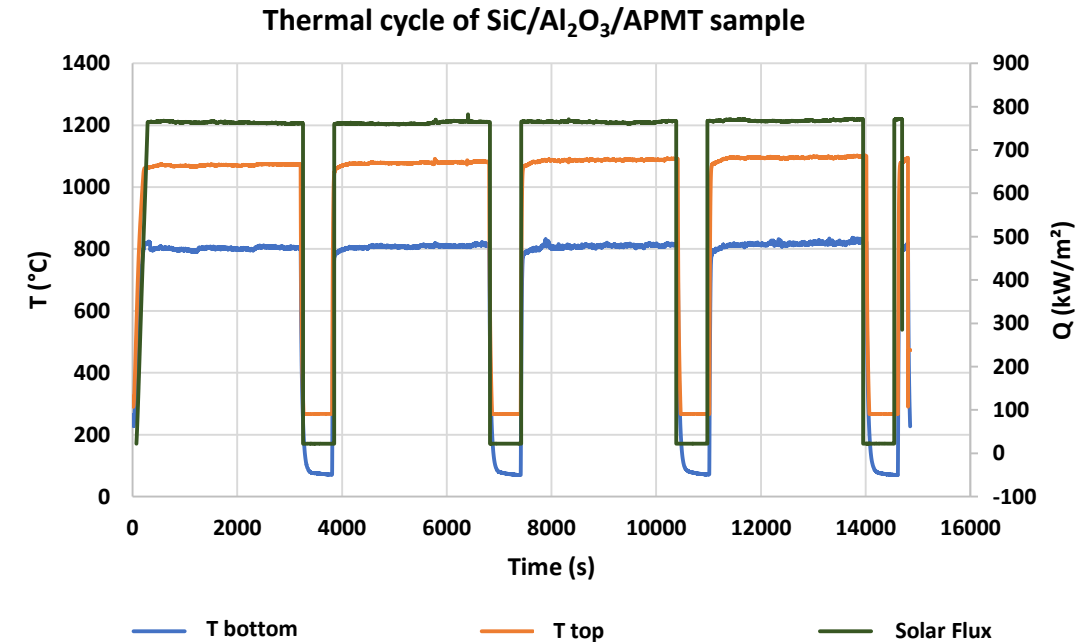
- Compressive stresses in both layers and methods
- **Numerical value of SiC is 23% lower than experimental value**
- For alumina the two values are very close (<5%)
- **Comparison with compression limits**
 - Observed cracks probably originate in alumina
 - Consequentially affect the SiC layer



□ After thermal cycle : SiC/Al₂O₃/APMT simple

➤ Simulation Parameters:

- Number of simulated cycles: **4**
- **1 hour** duration (**50 min** at high temperature and **10 min** rapid cooling)
- Incident solar flux: **800 kW/m²** → temperature reached at sample Top: **~1100 °C**
- Geometry and materials (multilayer):
 - ✓ Substrate: thickness: **2 mm**
 - ✓ Alumina (Al₂O₃) layer: **1 μm**
 - ✓ SiC layer: **10 μm**
- High SiC absorptivity: **81%**

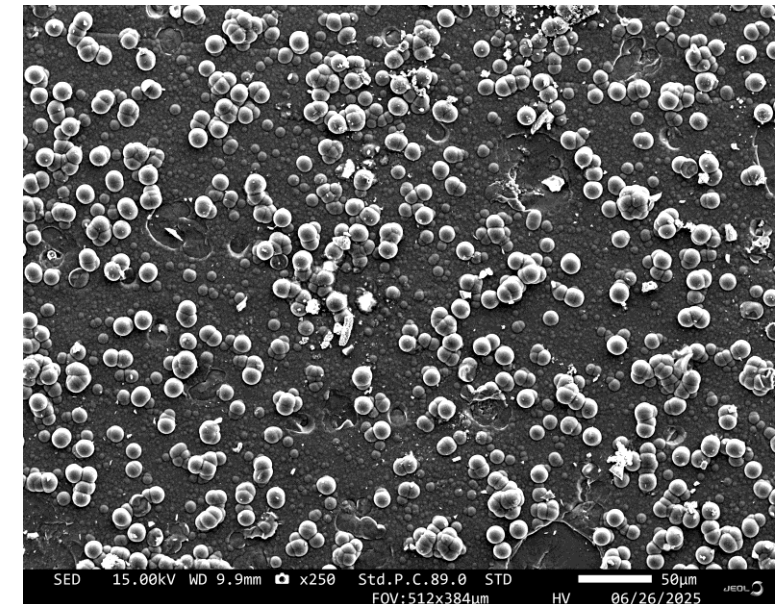


□ After thermal cycle : SiC/Al₂O₃/APMT sample

- **Oxidation observed:** confirmed by EDS and XRD analysis
- **Propagation of existing cracks.**

Layer	Numerical (MPa)	Experimental (MPa)	Limit compressive strength (MPa)
SiC	-2530	-1113	-2500 to -3500

- **Experimental stress is 50% lower than numerical stress**
 - DRX method is highly dispersive
- **Based on the results:** Numerical value reflects observations better (cracks and delamination)
- **Ongoing work: other methods**
 - Photoluminescence
 - Curvature measurement (Stoney)
- **Comparison of different methods**



- ❑ Simulations and experiments are very close for alumina but need correction for SiC layer
- ❑ Linear dependence between stress and deformation
- ❑ Some issues observed: delamination and crack propagation from alumina
- ❑ Promising concept, but needs **further optimization** for long-term stability

This work benefited from funding provided by the French State managed by the National Research Agency under the France 2030 program, reference ANR-22-PESP-0005.



Thank you for your attention

Thiane Ndiaye : thiane.ndiaye@cnrs.fr



UPR CNRS en
convention
avec l'UPVD



Annex 8: Residual Stress Measurement by X-ray Diffraction (XRD)

$$d_{hkl} = \frac{1+\nu}{E} \times \sigma \times d_0 \times \sin^2 \psi + \frac{-2 \times \nu}{E} \times \sigma \times d_0 + d_0$$

$$\frac{d_{hkl} - d_0}{d_0} = \frac{1+\nu}{E} \times \sigma \times \sin^2 \psi + \frac{-2 \times \nu}{E} \times \sigma$$

$$\varepsilon = \frac{d_{hkl} - d_0}{d_0} = \frac{1+\nu}{E} \times \sigma \times \sin^2 \psi + \frac{-2 \times \nu}{E} \times \sigma$$

$$\varepsilon = C \sin^2 \psi + D = f(\sin^2 \psi) \text{ where}$$

$$C = \frac{1+\nu}{E} \times \sigma \text{ and } D = \frac{-2 \times \nu}{E} \times \sigma$$

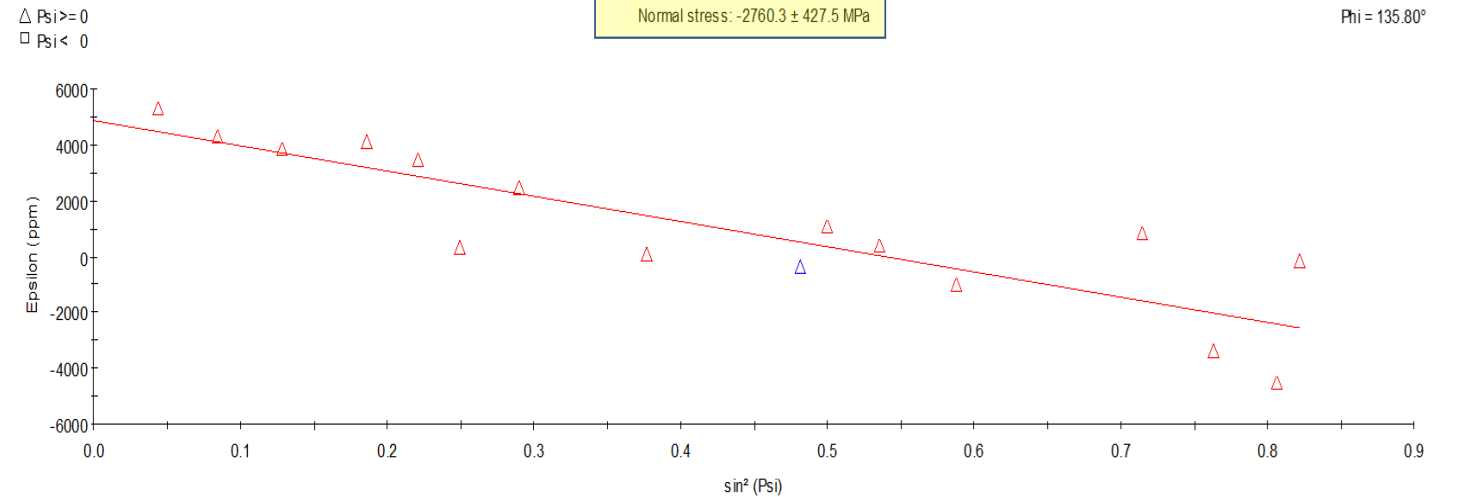
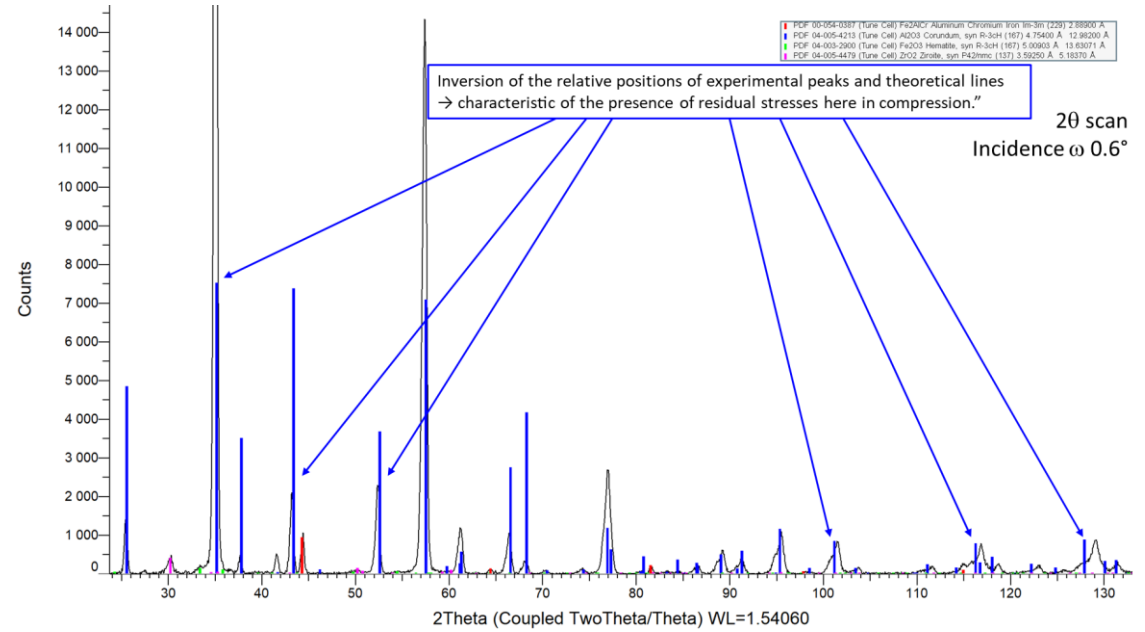
$$\sigma = \frac{E}{1+\nu} \times C$$

ε in the strain depending on ψ

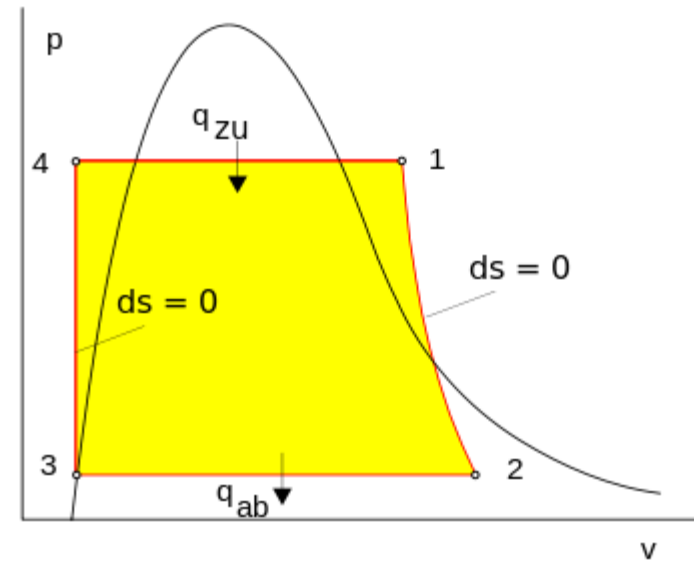
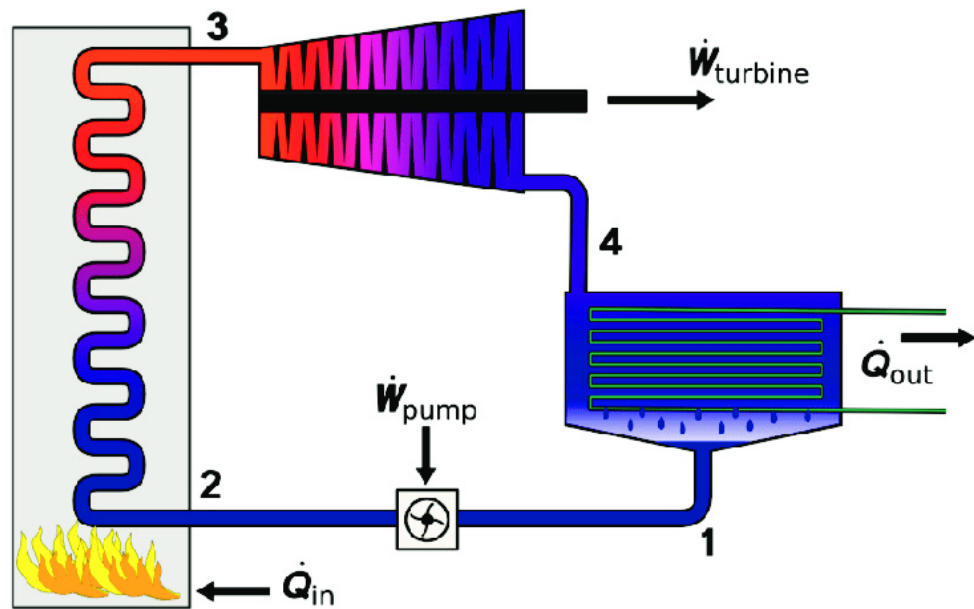
E is the Young Modulus

ν is the Poisson ratio

σ is the residual stress

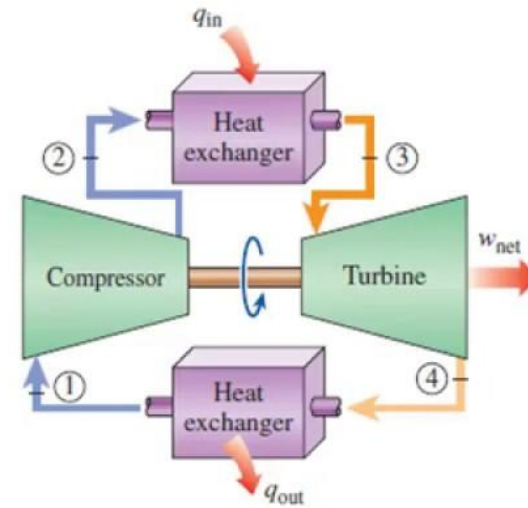
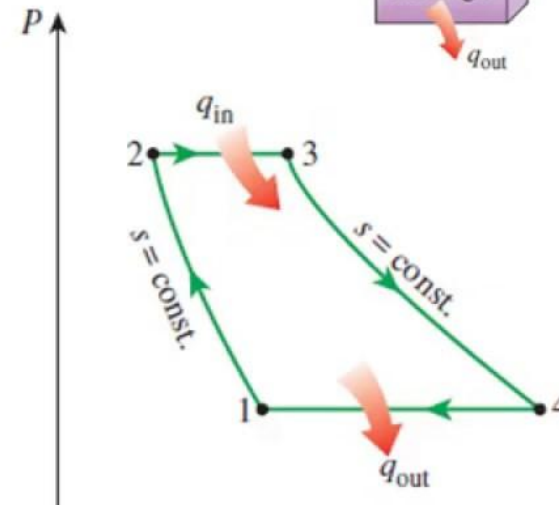
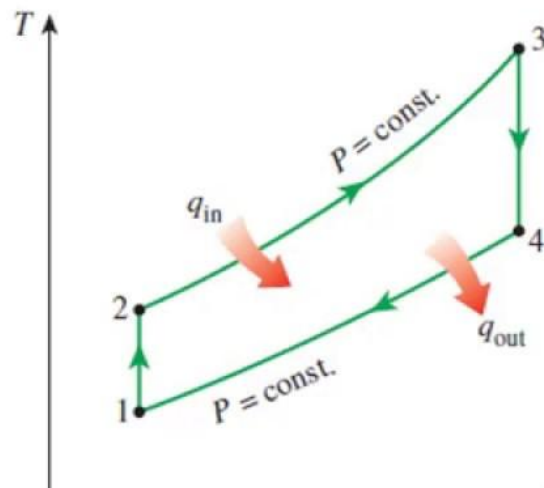


Annex 1: Rankine cycle

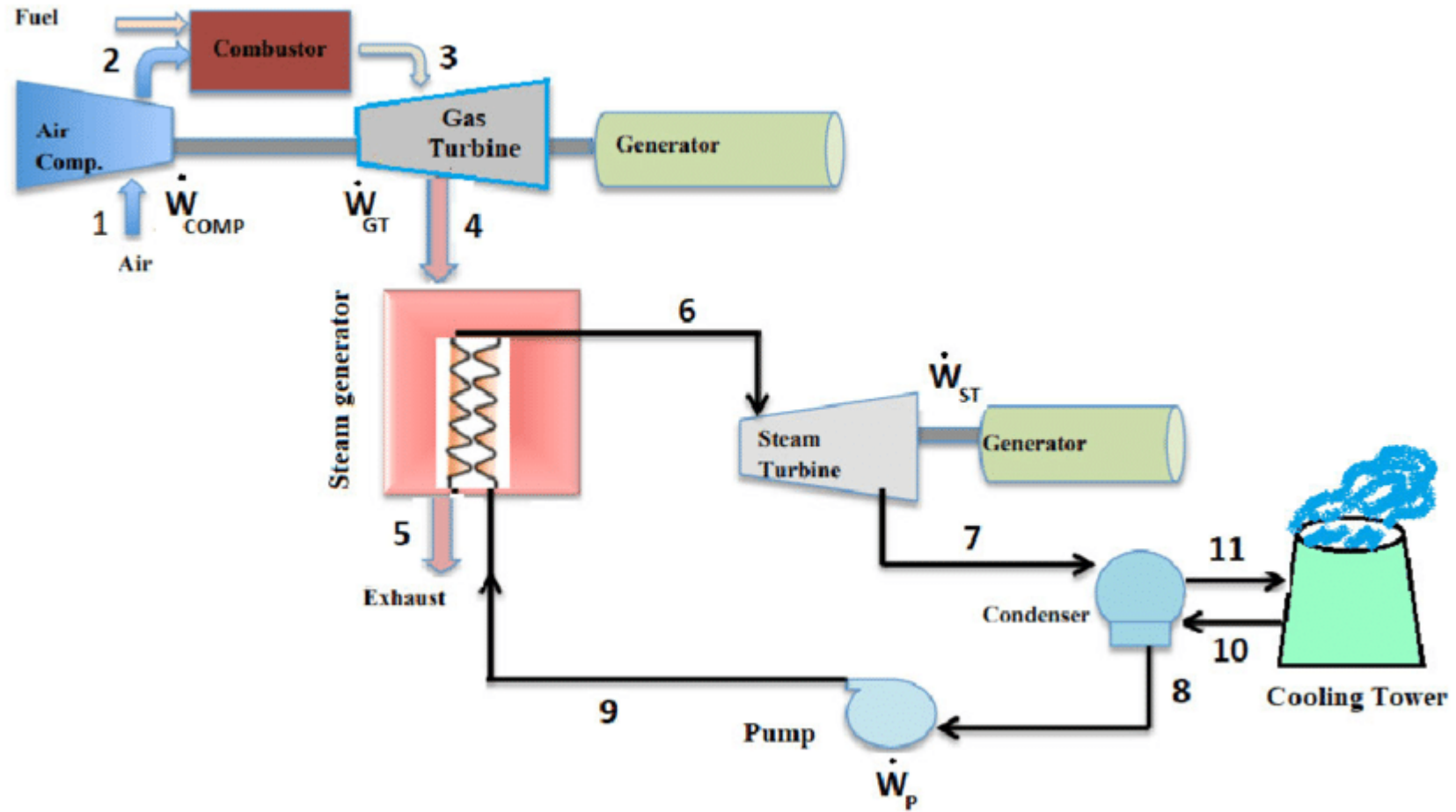


Annex 2: Brayton cycle

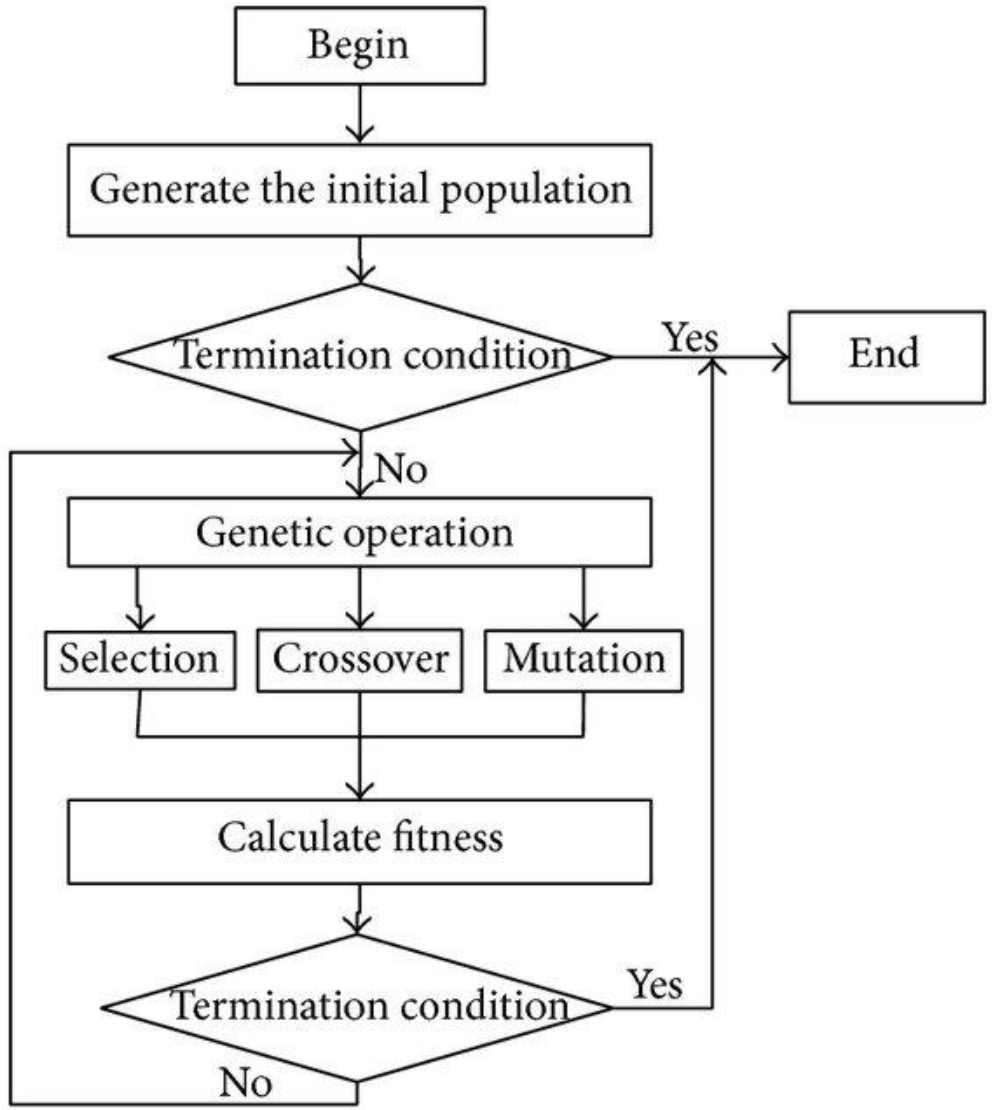
- 1-2 Isentropic compression (in a compressor)
- 2-3 Constant-**pressure** heat addition
- 3-4 Isentropic expansion (in a turbine)
- 4-1 Constant-**pressure** heat rejection



Annex 3: Combined cycle



Annex 4: Genetic algorithm



The resultant force due to the uniform strain component is zero

$$\begin{aligned}
 & \int_{z_{o,b}(t)}^{z_{c,bm}(t)} \frac{E_{o,b}}{1 - \nu_{o,b}} [c(z, t) - \varepsilon_{o,th,b}(z, t) - \varepsilon_{o,cr,b}(z, t) - \varepsilon_{o,l,b}(z, t)] dz \\
 & + \sum_{i=1}^m \int_{z_{c,b_i}(t)}^{z_{c,b_{i-1}}(t)} \frac{E_{c,b_i}}{1 - \nu_{c,b_i}} [c(z, t) - \varepsilon_{c,th,b_i}(z, t) - \varepsilon_{c,cr,b_i}(z, t) - \varepsilon_{o,g,b_i}(z, t)] dz \\
 & + \int_{-t_s \frac{t}{2}}^{\frac{t_s(t)}{2}} \frac{E_s}{1 - \nu_s} [c(z, t) - \varepsilon_{s,th}(z, t) - \varepsilon_{s,cr}(z, t)] dz \\
 & + \sum_{i=1}^m \int_{z_{c,t_{i-1}}(t)}^{z_{c,t_i}(t)} \frac{E_{c,t_i}}{1 - \nu_{c,t_i}} [c(z, t) - \varepsilon_{c,th,t_i}(z, t) - \varepsilon_{c,cr,t_i}(z, t) - \varepsilon_{o,g,t_i}(z, t)] dz \\
 & + \int_{z_{c,t_n}(t)}^{z_{o,t}(t)} \frac{E_{o,t}}{1 - \nu_{o,t}} [c(z, t) - \varepsilon_{o,th,t}(z, t) - \varepsilon_{o,cr,t}(z, t) - \varepsilon_{o,l,t}(z, t)] dz = 0
 \end{aligned}$$

The sum of bending component with respect to the bending axis is zero

$$\begin{aligned}
 & \int_{z_{o,b}(t)}^{z_{c,bm}(t)} \sigma_{o,b}(z, t) \cdot [z - t_b(t)] dz + \sum_{i=1}^m \int_{z_{c,b_i}(t)}^{z_{c,b_{i-1}}(t)} \sigma_{c,b_i}(z, t) \cdot [z - t_b(t)] dz \\
 & + \int_{-\frac{t_s(t)}{2}}^{\frac{t_s(t)}{2}} \sigma_s(z, t) \cdot [z - t_b(t)] dz + \sum_{i=1}^m \int_{z_{c,t_{i-1}}(t)}^{z_{c,t_i}(t)} \sigma_{c,t_i}(z, t) \cdot [z - t_b(t)] dz \\
 & + \int_{z_{c,t_n}(t)}^{z_{o,t}(t)} \sigma_{o,t}(z, t) \cdot [z - t_b(t)] dz = 0
 \end{aligned}$$

The resultant force due to the bending component is zero

$$\begin{aligned}
 & \int_{z_{o,b}(t)}^{z_{c,b_m}(t)} \frac{E_{o,b}}{1-\nu_{o,b}} \cdot \frac{z-t_b(t)}{r(t)} dz + \sum_{i=1}^m \int_{z_{c,b_i}(t)}^{z_{c,b_{i-1}}(t)} \frac{E_{c,b_i}}{1-\nu_{c,b_i}} \cdot \frac{z-t_b(t)}{r(t)} dz \\
 + & \int_{-\frac{t_s(t)}{2}}^{\frac{t_s(t)}{2}} \frac{E_s}{1-\nu_s} \cdot \frac{z-t_b(t)}{r(t)} dz + \sum_{i=1}^m \int_{z_{c,t_{i-1}}(t)}^{z_{c,t_i}(t)} \frac{E_{c,t_i}}{1-\nu_{c,t}} \cdot \frac{z-t_b(t)}{r(t)} dz \\
 + & \int_{z_{c,t_n}(t)}^{z_{o,t}(t)} \frac{E_{o,t}}{1-\nu_{o,t}} \cdot \frac{z-t_b(t)}{r(t)} dz = 0
 \end{aligned}$$